Advances in Science and Technology Research Journal

Advances in Science and Technology Research Journal, 2026, 20(4), 538–550
https://doi.org/10.12913/22998624/214462
ISSN 2299-8624, License CC-BY 4.0

Received: 2025.12.15
Accepted: 2026.01.19
Published: 2026.03.01

Influence of abrasive friction treatment on the structure of carbon steel taking into account its heat treatment

Valeriy Shevelya[1], Galyna Kalda[2,3], Mykhaylo Pashechko[4*], Oleksandr Dykha[1], Iuliia Sokolan[3]

[1] Department of Tribology, Automobiles and Materials Science, Khmelnitskiy National University, Instytutska Str. 11, 29016 Khmelnitskiy, Ukraine
[2] Department of Water Supply and Sewage Systems, Rzeszow University of Technology, al. Powstancow Warszawy 12, 35-959 Rzeszow, Poland
[3] Department of Construction and Civil Security, Khmelnitskiy National University, Instytutska Str. 11, 29016 Khmelnitskiy, Ukraine
[4] Department of Information Technology, Lublin University of Technology, ul. Nadbystrzycka 38, 20-618 Lublin, Poland
* Corresponding author's e-mail: mpashechko@hotmail.com

ABSTRACT

By methods of sclerometry (with registration of acoustic emission) and amplitude-independent internal friction the change of substructure and rheological and strength properties of carbon steel after heat treatment (hardening + tempering) and subsequent finishing-hardening friction treatment (abrasive grinding + polishing) has been investigated. Significant differences have been established in the change in the strength, rheological, and dissipative properties of martensite from the properties of medium and high tempered structures formed by friction processing. It is shown that, in contrast to highly tempered steel after abrasive impact, the degree of hardening of hardening of quenched martensite increases with increasing strain rate in scratch testing, indicating a different mechanism of strain hardening of these structures under friction treatment conditions. Exceptionally high acoustic-emission activity of hardening martensite (to 20 μm) caused by hardening treatment, as well as the rapid growth of the temperature background of internal friction, is due to the formation of ultradisperse (nanocrystalline) structure, which is characterized by high contact strength and relaxation capacity. Additional hardening of quenching martensite in the process of friction treatment, accompanied by an increase of relaxation resistance is caused by dynamic strain aging and dynamic stress tempering. The less pronounced acoustic-emission activity and low level of internal friction of tempering martensite (T_{temp} = 200 °C) indicate an increase in the elasticity of the structure with a decrease in the relaxation capacity, the level of which was stably maintained with a change in the speed of friction treatment. Highly tempered steel (T_{temp} = 600 °C) undergoes mechanical work hardening due to friction-activated surface plastic deformation, which is accompanied by a rapid decrease in dissipative (relaxation) capacity with the transfer of fracture processes under the friction surface. The analysis of experimental data is carried out in the context of the problem of creating wear-resistant materials, which at high strength should also have sufficient relaxation (damping) capacity.

Keywords: hardening, tempering, martensite, scratch testing, acoustic emission, internal friction, dynamic aging, friction machining.

INTRODUCTION

One of the effective ways to increase the reliability of friction units of machines is hardening treatment by intensive surface plastic deformation by impact and friction methods [1–3]. Impact surface plastic deformation is performed, for example, by chasing, shot blasting and bombardment with steel balls, vibro-impact treatment, etc. Friction methods of surface plastic deformation

include roller rolling, smoothing (including diamond smoothing), vibration grinding, mandrel grinding, sliding indenter or fixed abrasive processing, etc. [4–7]. Methods of friction processing are characterized by simplicity and sufficient efficiency of increasing the wear resistance of friction units.

One of the priority tasks of mechanical engineering is to improve and increase the efficiency of finishing operations of abrasive machining, which determine the geometric accuracy and operational properties of parts [8,9].

BACKGROUND

The whole variety of finishing and strengthening abrasive machining can be divided into methods of finishing with free and fixed abrasive [10,11]. The advantage of fixed abrasive is the possibility of smoothly changing the cutting ability of the tool in the process of finishing with the transition from coarse to finer surface finish.

In industry, grinding and polishing are traditional methods of finishing using abrasive tools. In grinding, plastic deformation and hardening of the surface layer occurs under conditions of impact interaction of abrasive grains with the material being processed [9,12,13]. Grinding as a method of abrasive finishing, in addition to ensuring high dimensional accuracy and optimal surface roughness, is designed to form high performance indicators of machine parts.

Grinding operation using non-rigid, flexible or elastic tools (abrasive elastic wheels, abrasive abrasives, abrasive belts, etc.) is widespread in finishing and strengthening of complex thin-walled parts [1,14]. Such parts, for example, are used in the aviation industry, where they strive to minimize the mass of products. For smoothing and polishing, friction machining in the regime of boundary friction with the use of abrasive sandpaper and polishing paste is usually applied.

In addition to removing allowances and forming optimal surface roughness, friction abrasive blasting is designed to improve the strength properties of parts operating under sliding and rolling friction. This is achieved by increasing hardness, fatigue strength, and by improving the corrosion resistance of parts made of alloy steels [15–17].

However, the wear resistance of steel is determined not only by hardness. For example, nanostructured friction treatment of hardened steel with a sliding indenter increased hardness by 40%, and wear resistance increased 2–3 times under conditions of adhesive and abrasive wear [5]. According to [6], after friction treatment (grinding + polishing) under conditions of "soft" wear under sliding friction without lubrication, hardened steel 45 showed almost an order of magnitude higher wear resistance compared to the sorbitic temper structure with only a threefold difference in hardness. This advantage of steel in the state of hardening increases with toughening of the friction regime. So, in comparison with normalized steel, hardened steel, which had three times higher hardness after friction treatment, showed 50–200 times higher wear resistance, which, in turn, depended on the load-velocity mode of friction. The effectiveness of the effect of surface plastic deformation during friction treatment on strain hardening and wear resistance decreases as the tempering temperature increases.

It is accepted [19–21] that the hardening of steel under severe surface plastic deformation occurs due to changes in the dislocation structure, crushing of grains and blocks, as well as due to the formation of residual compressive stresses in the surface layer. It is assumed that a more significant increase in the contact strength of martensite is associated with the connection of the transformation of residual austenite into martensite and the formation of nanocrystalline structure to the above structural factors [2,5]. However, at the substructural level, the role of diffusion-dislocation dynamic hardening processes during friction treatment of steel in connection with its initial structural state remains insufficiently studied. Moreover, there is an opinion [7] about the inexpediency of frictional surface plastic deformation in the manufacture of parts of friction units due to the possible appearance of overstressed areas with an excess of critical dislocation density, which leads to brittle fracture with the appearance of a large number of microcracks.

The majority of works devoted to abrasive machining, as a rule, focus on the optimization of abrasive tool composition to improve its performance characteristics, and also investigate the mechanism of chip formation and the effectiveness of coolant [8,18]. Fewer works are devoted to the study of substructural mechanisms of surface hardening of machined parts.

The aim of the article is to investigate metal physical aspects of dynamic transformation of

carbon steel substructure under conditions of finishing and strengthening abrasive (friction) treatment taking into account the initial structural state formed by heat treatment (hardening + tempering).

MATERAL AND EXPERIMENTAL PROCEDURE

Carbon steel 45 (0.47%C, 0.25%Si,0.65%Mn) in the state of hardening (in water from the temperature of 850 °C), as well as after tempering (within 1 hour) at temperatures of 100, 200, 400, 600 °C were studied. Accordingly, the steel hardness (HRC) was: 58, 54, 52, 41, 25. This steel is widely used in various industries for the manufacture of axles, crankshafts and camshafts, gears and gear wheels, plungers and other parts subject to increased wear. Two methods were used to study structural changes after thermal and abrasive friction treatment: sclerometric (scratch analysis) and the method of amplitude-independent (background) internal friction.

In the first case, friction treatment was carried out on a friction machine according to the scheme "finger-disk": the sample (finger) with a controlled force (P = 0.3 MPa; v = 0.25 m/s) was pressed against the plane of the rotating disk, on which abrasive sheets were fixed, periodically replaced in the process of triboactivation of the sample by a finer fixed abrasive. After grinding, the final stage of friction treatment was polishing using polishing paste.

Tribosclerometric and acoustic-emission properties of surfaces after hardening treatment were carried out on a scratch tester RST (Revetest Scratch Tester) manufactured by CSM Instruments (Switzerland). Sclerometry was carried out by continuous indentation of a Rockwell (up to maximal load F_N^{max} = 100 and 200 N) diamond indenter with simultaneous tangential movement of the sample relative to the indenter at a speed of 4 mm/min with a scanning base of 4 mm. In scratch testing, as the indenter deepened in a controlled manner, the following were recorded: normal load, sclerometric force and coefficient of friction, and acoustic emission. An indicator of the level of acoustic-emission activity (in %) was the integral acoustic emission caused by sound signals exceeding the set limitation threshold for the time interval under study. Laws of scratch testing, modeling local processes of interaction between a single abrasive grain and metal surface during sliding friction, contain information on the strength, viscoelastic and dissipative properties of friction contact.

To investigate the substructural changes caused by thermal and frictional treatment by the method of internal friction, a torsion pendulum-type setup described in [6] was used. The indicator of internal friction (dissipative capacity) was the logarithmic decrement of oscillations of the specimen (Figure 1a) subjected to frictional treatment at different speeds (0.08, 0.21, 0.34 m/s) on the unit, the schematic diagram of which is shown in Figure 1b. To construct temperature dependences of the internal friction background (relative strain $\gamma = 5 \cdot 10^{-5}$), heating was carried out by passing an electric current through a nichrome element covering a narrow working part of the specimen, the temperature of which was controlled by a thermocouple [6].

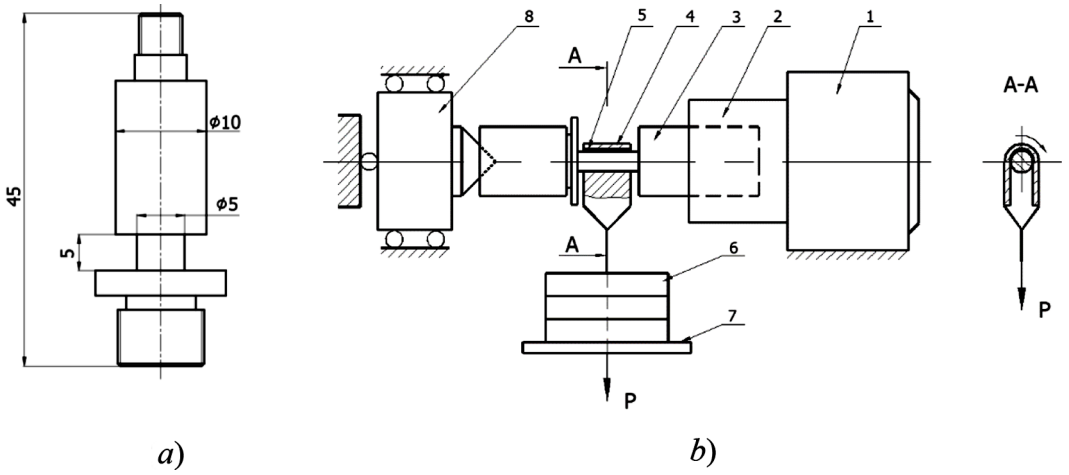

Figure 1. Specimen (a) and scheme of the friction machine (b)

The specimen 3, fixed in the clamp 2 and centering movable support 8, is driven into rotation at a predetermined speed by electric motor 1. Friction is carried out between the narrow working part of the specimen and abrasive pad 5 (P500), which is pressed with a controlled force to the cylindrical surface of the specimen covering fixture 4, which is loaded with weights 6, stacked on the suspension 7. Tests were carried out at a load $P = 10$ N and three sliding speeds: $v = 0.08$; 0.21; 0.34 m/s. The friction path was 300 m.

RESULTS AND DISCUSSION

Scratch analysis

The rheologic-dissipative performance of scratch-tested steel after thermal and subsequent friction treatment in relation to the acoustic-emission activity of the structure is illustrated in Figure 2.

The intensity of acoustic emission under mechanical loading of metal reflects the dynamics of local restructuring of the structure accompanied by relaxation of microstresses [22]. In this case, energy is released in the form of elastic (acoustic) waves with a change in the stress-strain state of the friction contact zone. Therefore, acoustic-emission activity caused by scratch testing can serve as an indicator of changes in the relaxation (dissipative) capacity of heat-treated steel under friction. The emergence of elastic waves under load accompanied by a sound effect is mainly caused by a sharp change in the velocity of dislocations (during their acceleration or deceleration).

Note that the hardened steel without friction treatment (after electropolishing) showed insignificant acoustic emission activity during sclerometry, which is caused by the low mobility of dislocations created by phase nucleation during hardening. The blocking of dislocations is due to the supersaturation of the solid solution with

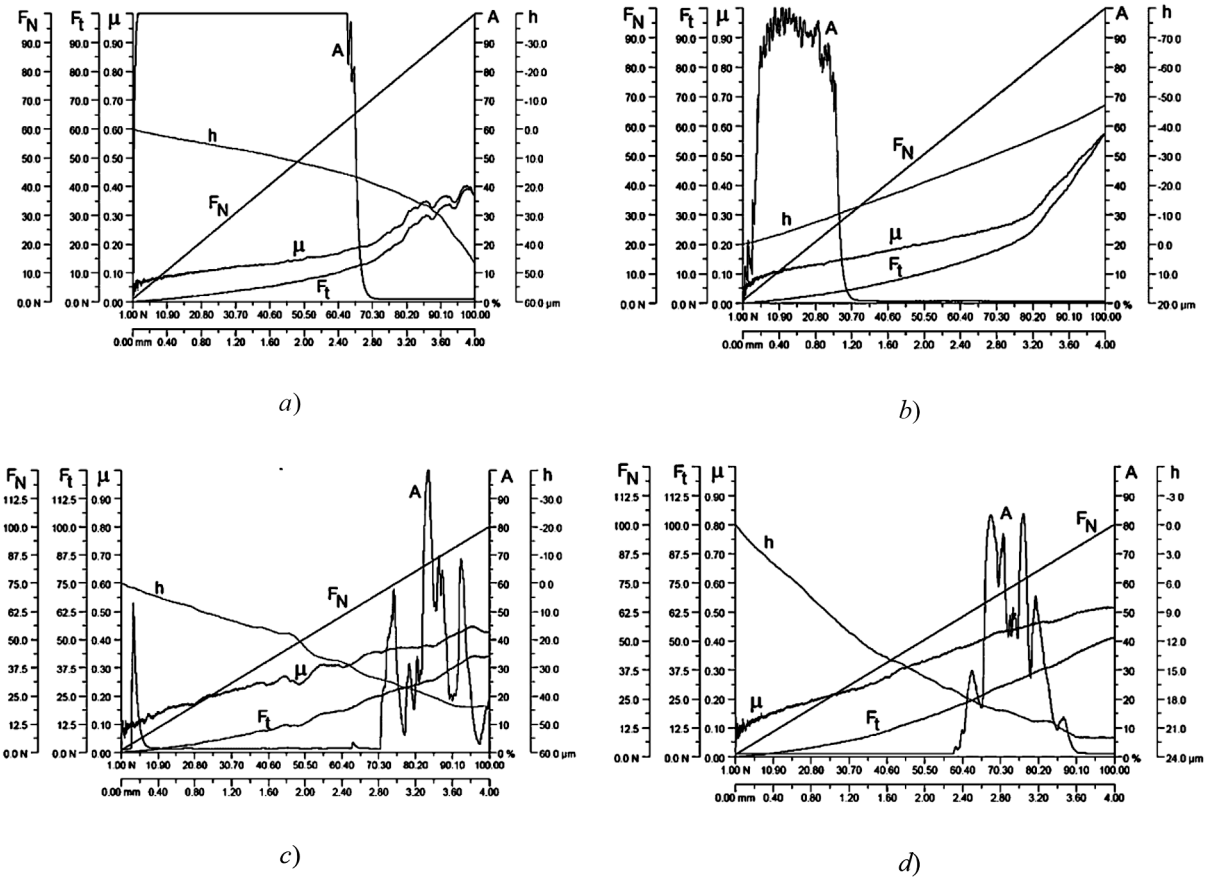

Figure 2. Sclerometric indices of friction-treated steel 45 depending on the preliminary heat treatment conditions: *a* – hardening; *b*, *c*, *d* – tempering temperature, respectively, 200, 400, 600 °C; F_N – normal load, N; F_t – friction force, N; μ – friction coefficient; A – acoustic emission, %; h – depth of indenter penetration, μm (indenter loading speed v_F = 100 N/min, F_N^{max} =100 N)

carbon and high local microstresses. However, after friction treatment (grinding + mechanical polishing), the hardening martensite showed exceptionally high acoustic-emission activity of the near-surface layer up to 20 μm deep due to the formation of an ultradisperse structure (Figure 2a). During scratch testing of such a structure, dynamic stress relaxation (damping) is enhanced by the mechanism of viscous flow along grain and block boundaries (boundary relaxation), which causes an increased acoustic effect. Low-temperature tempering (T_{temp} = 200 °C) significantly reduces the intensity of acoustic emission initiated by friction treatment, although the near-surface localization of acoustic activity of tempered martensite remains (Figure 2b).

Tempering of steel at higher temperatures, significantly reducing the intensity of acoustic emission, leads to a shift of its manifestation areas to deeper friction-activated layers (Figure 2c,d). Figure 3 shows the change in the level of acoustic emission and sclerometric friction force as a function of tempering temperature after thermal and friction treatments of steel.

By the nature of changes in the force and friction coefficient in the process of scanning and indenter embedding (see Figure 2), in all cases a hardening zone formed by friction machining and a zone (at a certain depth) of the original structure not activated by the abrasive impact are revealed. The maximum values of sclerometric friction force associated with the depth of indenter penetration and registered within the indicated zones are shown in Figure 3 (curves 2 and 3). Curve 2 characterizes the degree of surface hardening of steel after thermal and friction treatments, and curve 3 shows that the friction force changes accordingly to the change in the modulus of elasticity of steel depending on the tempering temperature [6]. The growth of elasticity of low tempered martensite (T_{temp} = 100, 200 °C), caused by the release of ε-carbides, is the reason for the decrease in acoustic activity with a decrease in the depth of its manifestation to 5–10 μm (Figure 2b).

The microstructure rearrangement accompanied by powerful acoustic pulses during scratch testing of triboactivated martensite (Figure 2,3) is caused by a number of discrete dynamic relaxation processes that reduce the probability of brittle fracture [23,24]:

- accelerated movement of dislocation loops at mass detachment from anchoring points formed by ultradisperse structure and dynamic strain aging;
- breakthrough by dislocation clusters of carbide precipitates created by dynamic tempering;
- microplastic deformation by twinning as the density of twins grows, providing more efficient stress relaxation than sliding.

The level of acoustic emission depends to a greater extent not on the dislocation density, but on the dynamics of their motion and the length of free accelerated travel. Therefore, highly

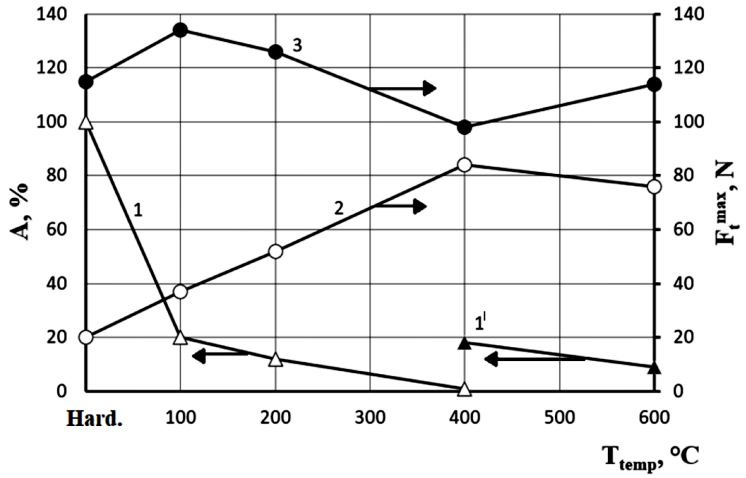

Figure 3. The influence of preliminary tempering temperature of friction-treated steel on the level of acoustic emission *A* (1,1′) and maximum values of sclerometric friction force during simultaneous indentation F_t^{max} (2,3): v_F = 200 N/min; F_N^{max} = 200 N; 1 and 1′ – acoustic activity, respectively, of the friction surface and subsurface layers (*h* = 20–40 μm); 2 – at the boundary of the friction hardened zone; 3 - outside the influence of FT at F_N^{max} = 200 N

tempered steel (T_{temp} > 400 °C) due to low potential deformation barrier under friction conditions is subjected to mechanical sticking with high density of slow-moving dislocations, when their motion is blocked by a large number of barriers; simultaneously, the work of free dislocation sources is suppressed. As a consequence, the relaxation ability of the material falls sharply, as evidenced by the tendency to zero acoustic emission in the layers immediately adjacent to the friction surface. The acoustic emission registered in deeper layers (Figure 2c,d), apparently, is caused by the formation of free interfaces like relaxation microcracks.

Studies [24,25] have shown that the sclerometric parameters of the studied structures depend on the indenter loading rate. This concerns both the localization of the regions of increased acoustic emission and the indenter embedding rate (increment of the indenter embedding depth per unit load, Figure 4).

It can be seen that in case of scratch analysis of highly tempered steel, the increase in the rate of force applied to the indenter was accompanied by a corresponding increase in the rate of its immersion. In the case of hardened and low-tempered steel (hardening martensite and tempering martensite), the opposite phenomenon was observed: the rate of indenter embedding, which characterizes the pliability of the structure, decreased with the increase in the rate of its loading. i.e., the degree of strain hardening of martensite increases with the increase in the strain rate. This may be an indication that the strain hardening of the frictional contact of these structures differs both in mechanism and efficiency.

It is known that surface intense plastic deformation by friction is an effective way to refine the grain structure of metals to nanoscale [19,20]. This is facilitated by a high degree and rate of multidirectional hot deformation (shear compression) accompanied by dynamic recrystallization in a certain temperature range. As a result, a gradient structure with grain fragmentation from micro- to submicro- and nanoscale levels is formed in the surface layer during friction.

It was found [19] that after intense plastic deformation by friction of armco-iron, a decrease in grain size from coarse-crystalline to micro- and submicron sizes (up to 100–200 nm) is accompanied by an increase in hardness and a decrease in plasticity with a stable value of Young's modulus of elasticity. However, a further decrease of grain sizes (from 100 to 20 nm), on the contrary, causes some decrease in hardness and elastic modulus with an increase in the microplasticity of the nanostructure.

According to the existing ideas [19,20], the grain boundaries and boundary regions play a determining role in the decrease of elastic properties and unstrengthening of nanostructures (d < 100 nm), the volume fraction of which increases as the grain size decreases. Therefore, in nanostructures it becomes energetically more

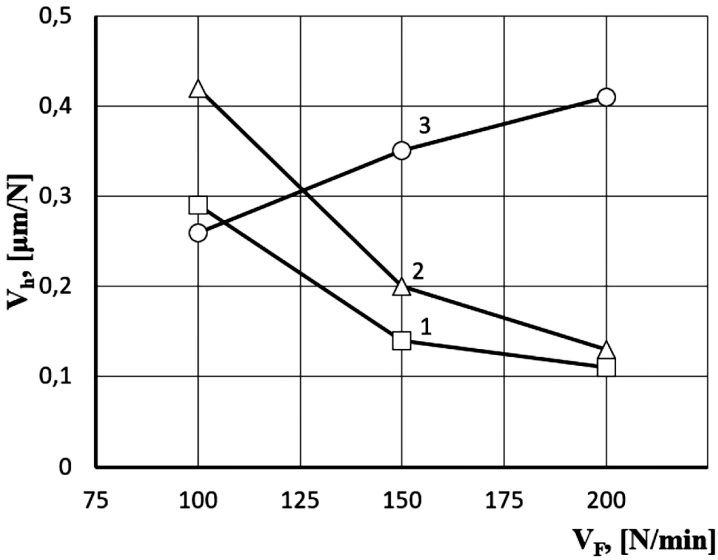

Figure 4. Influence of vertical indenter loading rate V_F during surface scanning on its penetration rate V_h: 1 – hardening; 2 – T_{temp} = 200 °C; 3 – T_{temp} = 600 °C

advantageous to connect to the relay dislocation mechanism of deformation (with the transmission of slip across grain boundaries) the mechanism of grain boundary slip with the activation of rotational modes of deformation. Thus, the de-strengthening of nanostructures ($d \leq 50$ nm) is due to a change in the plastic deformation mechanism compared to a larger grain structure. Apparently, for this reason, the finer-grained martensite nanostructure at an indenter loading rate of 100 N/min shows greater ductility compared to highly tempered steel. However, with an increase in the deformation rate, the degree of martensite hardening increases, and the softening factor of grain boundary sliding has less of an effect.

Internal friction method

The differences in the fine crystal structure of the heat-treated samples (Figure 1a), as well as the structure formed during friction treatment at the unit shown in Figure 1b, were studied by the method of amplitude-independent (background) internal friction [26]. The results of the study are shown in Figure 5,6.

Figure 5 shows the effect of heat treatment of steel on the temperature dependences of the logarithmic decrement of attenuation, which is mainly due to mechanical losses at vibrations of dislocation segments, the sizes of which depend on the degree of anchoring of dislocations by impurity atoms of introduction (C+N). In addition, the background of internal friction is affected by diffusive creep and boundary relaxation caused by viscous flow along interfaces (grains, blocks, etc.) under force and thermal activation.

On the temperature dependences of internal friction (IF) of steel in the initial states of hardening and low tempering (Figure 5, curves 1,2), relaxation maxima are formed in the region of temperatures 60 and 80 °C, which correspond, respectively, to nitrogen and carbon peaks of internal friction [26]. The temperatures at which these internal friction peaks are formed are determined by the frequency of the excited freely damped oscillations of the sample (in our experiments $f \sim 60$ Hz). Nitrogen and carbon atoms, as introducing impurities, are in octahedral positions, creating tetragonal distortions in the VCC lattice. At a certain temperature and frequency of action of periodic loading in the stress field there is a sharp increase in the migration of introduced atoms along the inter-nodes of the crystal lattice. Such activation of diffusion redistribution of impurity atoms leads to resonant growth of energy dissipation (mechanical losses) with formation of relaxation maxima of internal friction (Snook peaks), the height of which is proportional to the concentration of introduction atoms in the solid solution. However, in deformed steel they can disappear after deformation or thermal aging at temperatures above 100 °C [26,27].

The weak temperature dependence of the damping decrement of tempered martensite

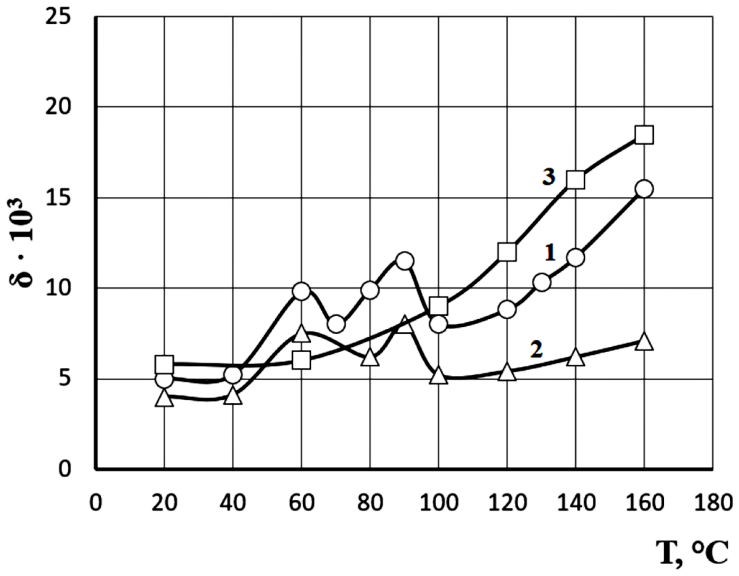

Figure 5. Influence of steel heat treatment on temperature dependences of internal friction background after friction treatment ($f \approx 60$ Hz; $\gamma = 5 \cdot 10^{-5}$): 1 – hardening; 2 – $T_{temp} = 200$ °C; 3 – $T_{temp} = 600$ °C

(Figure 5, curve 2) is associated with the release of fine ε-carbide particles coherently bound to the matrix and limiting the mobility of dislocation segments. At the same time, after high-temperature tempering (Figure 5, curve 3), with increasing temperature, the mobility of dislocation segments and diffusive creep along the interfaces increase more significantly due to a significant decrease in the concentration of impurity atoms (C+N) in the solid solution and changes in the morphology of carbide separations after tempering [28].

The character of changes in the intensity of vibration attenuation of samples after friction treatment with increasing temperature depend not only on the structural state of steel, but also on the speed of friction treatment (Figure 6). The disappearance of Snook relaxation after friction indicates the departure of impurity atoms from solid solution to dislocations or to carbides.

From all investigated structures of heat-treated steel and after all given speeds of friction treatment, hardening martensite showed in the temperature range 20–160 °C the greatest dissipative (relaxation) capacity (Figure 6, curves 1). This distinctive feature of hardened steel is most characteristic of the reduced friction velocities: v = 0.08; 0.21 m/s (Figure 6a,c). Low tempering of steel (T_{temp} = 200 °C) causes a sharp decrease in both the level of dissipative capacity and its temperature dependence (Figure 6, curves 2).

The change in the relaxation ability of steel was evaluated by the average temperature coefficient of energy dissipation: $\alpha_T = \Delta\delta/\delta_0 \cdot \Delta T$ (relative increase in the decrement of attenuation per one degree of temperature increase), which characterizes the degree of blocking and mobility of dislocations under conditions of thermomechanical activation (Figure 7). The values of $\Delta\delta$ were determined in the temperature range ΔT = 40–140 °C. The larger α_T is, the more easily dislocations detach from blocking impurity atoms and carbide precipitates under cyclic loading and the less resistance to viscous flow along grain boundaries and separated phases occurs with increasing temperature.

Discussion of research results

The high-temperature tempered steel (T_{temp} = 600 °C) is characterized by a progressive decrease in α_T with increasing friction velocity (Figure 7, curve 3), which is due to the formation of a low-mobility dislocation structure with a reduction in the distance between the attachment points in the dislocation network (L_N) and a decrease in the length and mobility of dislocation segments (L_C) formed by weaker attachment centers. In contrast to the high-temperature tempering structure, the initial growth of the thermal index α_T after friction treatment in the velocity range of 0.08...0.21 m/s with its subsequent decrease with increasing velocity up to 0.34 m/s is characteristic, albeit to a different degree, for hardening martensite and tempering martensite (T_{temp} = 200 °C) (Figure 7, curves 1 and 2).

The significant initial increase in the α_T coefficient at friction of hardening martensite can be caused by several reasons (Figure 7, curve 1). Hardening of steel produces a high density of hardening vacancies, which concentrate predominantly at grain and block boundaries, which are both sources and sinks of these point defects. Migration of vacancies along the interfaces in the field of cyclic stresses contributes to the growth of diffusive creep (boundary relaxation), the efficiency of which is manifested the higher the more fine-grained the structure [26]. Taking into account that in the process of friction hardening martensite, a highly dispersed (nanocrystalline) cellular structure is formed in the near-surface layer [5], diffusive creep is further facilitated and the rate of viscous flow along grain, block, and twin boundary surfaces increases. This leads to a sharp increase in the temperature dependence of the internal friction background and dissipative capacity of steel (Figure 6, curve 1).

Another reason for the initial increase in the α_T coefficient during friction of hardening martensite is the high density of mobile dislocations associated with easier, thermally activated, detachment of dislocation segments from the anchoring centers formed by (C+N) impurities. Moreover, the concentration of such centers in the process of friction martensite decreases due to the decomposition of the latter, when with the formation of ε-carbides the percentage of carbon in the solid solution decreases, which leads to an increase in the length of dislocation segments with a corresponding increase in microplasticity and dissipative (relaxation) ability of steel. Apparently, at the same time phase accretion and tetragonality of the lattice are reduced, and the work of dislocation sources is activated.

When the sliding velocity increases up to v = 0.34 m/s, causing an increase in the contact temperature and dislocation movement velocity,

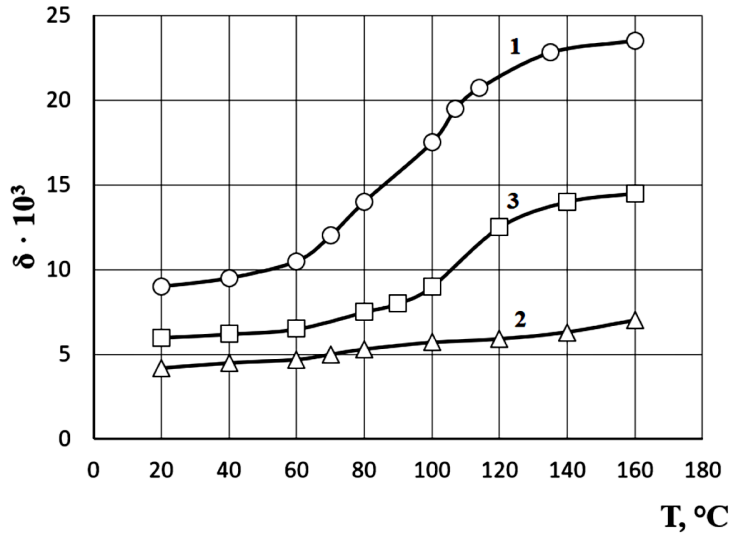

a)

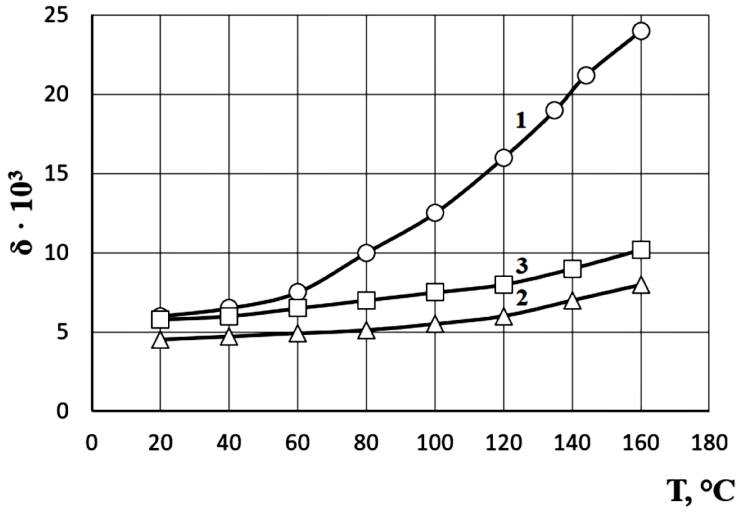

b)

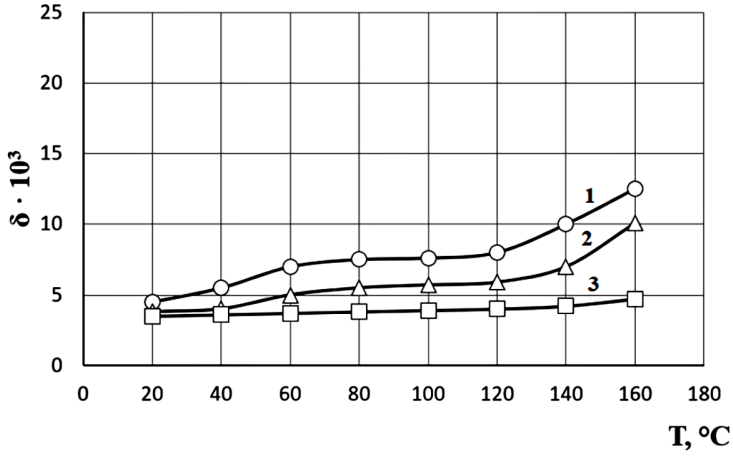

c)

Figure 6. Influence of steel heat treatment and speed of subsequent abrasive friction treatment on temperature dependences of internal friction background (contact load P = 10 N; friction path L = 300 m): *a* – v = 0.08 m/s; *b* – v = 0.21 m/s; *c* – v = 0.34 m/s; 1 – hardening; 2 – T_{temp} = 200 °C; 3 – T_{temp} = 600 °

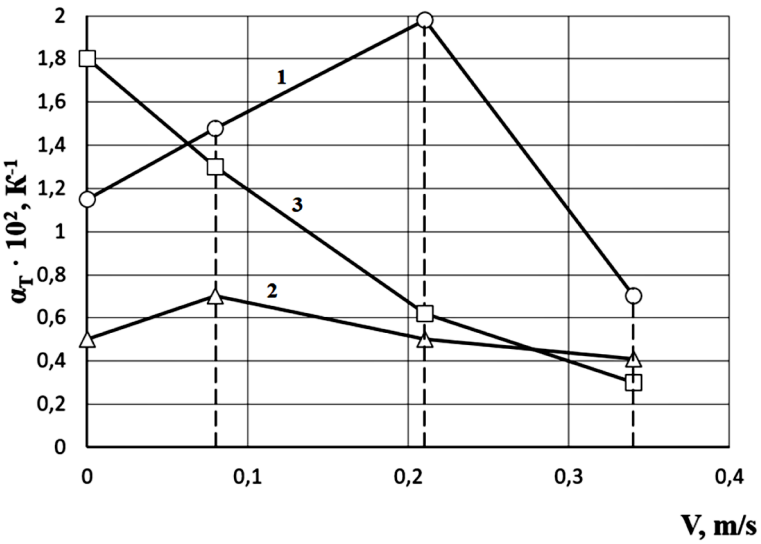

Figure 7. Influence of friction rate and heat treatment of steel on the temperature coefficient of energy dissipation: 1 – hardening; 2 – T_{temp} = 200 °C; 3 – T_{temp} = 600 °C

dynamic strain aging is activated in the frictional contact zone, accompanied by an increase in the degree of anchoring of dislocations by impurity atoms (C+N) [29,30]. The energy and thermal stability of the bonding of dislocations with impurity atoms and their atmospheres increases. The dissipative capacity of the structure under dynamic strain aging decreases due to the reduction in the length of dislocation segments and a decrease in the total mobility of dislocations. Optimal conditions for the development of dynamic strain aging are created at such friction velocities and temperatures, when the velocity of dislocation motion becomes commensurate with the diffusion velocity of impurity atoms. Judging by the intensity of the decrease in the α_T index with increasing external friction velocity (Figure 7, curve 1), the hardened steel is subject to significant additional hardening under the studied conditions. Hardening, forming a metastable structure with a high concentration of impurity atoms (C+N) in the solid solution, contributes to the enhancement of the effect of dynamic deformation aging under friction.

Simultaneously with dynamic strain aging, martensite decomposition and transformation of residual austenite with the release of highly dispersed carbide particles are accelerated. These processes are associated with the so-called stress tempering (dynamic tempering), which is accompanied by structural relaxation due to diffusive redistribution of impurity atoms with the formation of new phases [31,32]. Dynamic tempering contributes to the growth of hardening efficiency due to the formation of highly dispersed carbides, which create an additional barrier effect for dislocations. Compared to conventional tempering, dynamic tempering under load results in a more complete decomposition of martensite, which provides an additional increase in the strength of dislocation attachment, and the temperature forming the maximum elastic limit is 50...100 °C lower. On the other hand, carbide particles favorably affect the relaxation ability of the material, because they promote the generation of fresh dislocations during friction and cause a decrease in the concentration of carbon in the matrix, which leads to a decrease in the density of dislocation attachment points.

Thus, the hardening of friction hardening martensite is caused by the processes of dynamic strain aging and dynamic tempering, which are associated with stress relaxation due to:

- diffusion redistribution of carbon and nitrogen atoms in the field of cyclic stresses, as well as displacement of weakly fixed dislocations;
- structural relaxation (physicochemical reactions of decomposition of supersaturated solid solution – martensite and transformation of residual austenite).

It is necessary to add the above-mentioned dynamic relaxation processes caused by discrete accelerated motion of dislocations associated with the formation of ultradisperse structure during friction and the growth of twin density.

Tempered martensite (T_{temp} = 200 °C) shows the lowest ability to dissipate mechanical energy and the greatest temperature stability of relaxation resistance at changing sliding velocity (Figure 6,7, curves 2). Already in the process of low-temperature tempering there is a significant decrease in internal friction due to the decomposition of martensite with the release of highly dispersed ε-carbide particles coherently bound to the matrix [6]. Simultaneously, the transformation of residual austenite occurs with the formation of low-carbon martensite and dispersed carbides. Although a high density of dislocations remains in the twin crystals of martensite, they are anchored by atmospheres of impurity atoms of introduction and separated carbides. As a result, the mobility of dislocations is minimized and the structure acquires high elasticity and relaxation resistance. Due to the high elasticity of such steel, the increase in the number of dislocations in the friction process is small and only additional dynamic aging occurs during DSA.

Steel in the state of low-temperature tempering (tempered martensite), possessing high elasticity, in friction is less susceptible to nanostructuring processes, which would effectively contribute to the manifestation of diffusion creep and, consequently, the growth of the background of internal friction (Figure 6, curve 2). The low level of internal friction of such steel, which does not change much with increasing temperature, is also due to the low ability of dislocations to creep due to a decrease in the mobility of vacancies during the formation of vacancy-impurity atom complexes [26]. The dislocations are fixed to such an extent that the process of their detachment both in the initial state and after friction is thermally weakly activated in the range of investigated temperatures and friction velocities, which causes low values and small variability of α_T (Figure 7, curve 2).

Highly tempered steel (T_{temp} = 600 °C) is characterized by a reduction in the thermal dissipation coefficient α_T with increasing friction velocity (Figure 7, curve 3). In this case, the temperature dependences of the internal friction background (Figure 6), characterizing the mobility of dislocations, are determined by the competition of two mechanisms of their detachment according to two types of stoppers - dislocation mesh nodes and weaker anchoring centers - impurity atoms and carbide precipitates [33]. With increasing friction velocity of highly tempered steel, the degree of mechanical sticking increases mainly due to the increase in the degree of dislocation attachment by dislocation "forest" nodes, which can significantly mask the processes of detachment of dislocation segments from weaker attachment centers. At such mechanical accretion of steel, the relaxation (dissipative) capacity of the structure is significantly reduced, which adversely affects the wear resistance [6].

CONCLUSIONS

By methods of sclerometry and amplitude-independent internal friction the influence of heat treatment of carbon steel and subsequent finishing-hardening abrasive friction treatment on substructural changes and rheological and strength properties has been investigated. It has been established that the degree of hardening and change of relaxation ability of hardened steel depends on tempering temperature and load-velocity mode of friction treatment.

Scratch analysis with continuous indenter indentation and acoustic emission registration showed significant differences in the change of strength, rheological and dissipative parameters of martensite from the properties of medium and high tempering structures formed by friction treatment. It is shown that in contrast to high-tempered steel (T_{temp} = 600 °C) after abrasive impact the degree of hardening of martensite increases with increasing strain rate in scratch testing, indicating the difference in the mechanisms of strain hardening of these structures under conditions of friction treatment.

Exceptionally high acoustic-emission activity (to a depth of 15–20 μm) of hardening martensite caused by hardening treatment has been established, which is due to the formation of an ultradisperse (nanocrystalline) structure characterized by high contact strength and relaxation capacity. Additional hardening of hardening martensite during friction treatment is caused by dynamic strain aging and dynamic tempering (stress tempering), which is facilitated by the metastability of the structure with a high concentration of impurity atoms (C+N) and hardening vacancies.

Nanostructuring of hardening martensite in the process of hardening treatment promotes activation of boundary relaxation and diffusive creep under dynamic loading conditions, which

is confirmed by the growth of the temperature background of internal friction after friction treatment in the speed range of 0.1–0.2 m/s. Further increase of processing speed is accompanied by growth of relaxation resistance of structure with decrease of mechanical losses due to development of strengthening dynamic processes of deformation aging and stress tempering. Diffusion-dislocation hardening mechanisms accompanied by dynamic relaxation phenomena reducing the probability of brittle fracture are considered.

It is shown that low-tempered tempered steel – tempering martensite (T_{temp} = 200 °C) after friction treatment shows reduced acoustic-emission activity, which is associated with the growth of elasticity and relaxation resistance of the structure due to the release of ε-carbides both at the stage of preliminary heat treatment and in the process of friction treatment. Under abrasive action, this leads to a decrease in the depth and degree of dispersion of the surface layer, and significantly increases and stabilizes the relaxation resistance compared to hardening martensite.

Zero surface acoustic-emission activity of friction-treated medium- and high-tempered structures has been established, which indicates low relaxation ability with a high degree of mechanical sticking causing subsurface destruction at a depth of 20–30 microns. The level of dissipation of mechanical energy (internal friction) of such steel, characterizing relaxation properties, rapidly decreases with increasing speed of friction processing.

REFERENCES

1. Evdokimov V.D., Klimenko L.P., Evdokimova A.N. Technology of Hardening of Engineering Materials. Kyiv: Professional, 2006.
2. Lu K., Lu J. Nanostructured surface layer on metallic materials induced by surface mechanical attrition treatment. Mat. Sci. Eng. A. 2004; 375–377: 38–45.
3. Deng S.Q., Godfrey A., Liu W., Zhang C.L. Microstructural evolution of pure copper subjected to friction sliding deformation at room temperature. Mat. Sci. Eng. A. 2015; 639: 448–455.
4. Baraz V.R., Fedorenko O.N. Features of frictional processing of steels of the spring class. MiTOM 2015; 11: 16–19.
5. Makarov A.V., Korshunov L.G. Metallophysical foundations of nanostructuring frictional processing. FMM 2019; 120(3): 327–336.
6. Shevelya V., Pashechko M., Kalda G., Sokolan Yu. Dynamic processes of substructural rearrangement under friction of carbon steel. Advances in Science and Technology Research Journal 2023; 17(3): 236–248.
7. Pinchuk V.G., Korotkevich S.V., Bobovich S.O. Influence of preliminary deformation by rolling on the processes of destruction of the surface layer of nickel during friction. Heavy Engineering 2010; 2: 23–27.
8. Kurdyukov V. Fundamentals of abrasive processing, 2014.
9. Pandiyan V., Shevchik S., Wasmer K., Castagne S., Tjahjowidodo T. Modelling and monitoring of abrasive finishing processes using artificial intelligence techniques: A review manuscript 2022: 138.
10. Starosta R. Obróbka powierzchniowa. Wyd. Akademii Morskiej w Gdyni, 2008.
11. Bańkowski D., Spadło S. The aplication of vibro-abrasive machining for smoothing of castings. Archives of Foundry Engineering 2017; 17(1): 169–173.
12. Shumyacher V.M. Physical and chemical processes during finishing. Volg.GASU, Volgograd, 2004.
13. Kacalak W., Tandecka K. Effect of Superfinishing methods kinematic features in the machined surfaces. J. Machine Engineering 2012; 4: 35–48.
14. Stepanov D.N. Finishing of thin-walled and complex-profile parts. report 1. Analysis of finishing-decorating methods. New Materials and Technologies in Metallurgy and Mechanical Engineering 2015; 1: 122–125.
15. Baron Yu.M. Influence of magnetic and magnetic-abrasive treatment on the phase composition and structure of the surface layer of tool steels. Electrophysical and Electrochemical Processing Methods 2012; 4(70): 12–17.
16. Akulovich L.M., Sergeev L.E., Shabunya V.V., Dubnovitsky S.K. Corrosion resistance of parts made of alloyed steels after magnetic-abrasive treatment. Industry. Applied Science. Materials Science 2018; 11: 45–50.
17. Boguslaev V.A., Kachan A.Ya., Mozgovoy V.F. Finishing technologies for processing GTE parts. Vestnik Dvigatelestroeniya 2009; 1: 71–78.
18. Abrasive Processing, Abrasive Tools and Materials. Materials of Articles of the XVII International Scientific and Technical Conference, Volgograd 2019.
19. Yurkova A.I., Milman Yu.V., Byakova A.V. Structure and mechanical properties of iron after surface severe plastic deformation by friction. I. features of the formation of the structure. Deformation and Destruction of Materials 2009; 1: 2–12.
20. Swygenhoven H.V., Weertman J.R. Deformation in Nanocrystalline Metals. Materialstoday 2006; 9(5): 24–31.

21. Estrin Y., Vinogradov A. Extreme grain refinement by sever plastic deformation. A Wealth Challenging Science Acta Mater 2013; 51: 782–817.
22. Semashko N.A., Shport V.I., Maryin B.N. Acoustic emission in experimental materials science. M.: Mashinostroenie, 2002.
23. Hase A., Mishina H., Wada M. Correlation between features of acoustic emission signals and mechanical wear mechanisms. Wear 2012; 292: 144–150.
24. Shevelya V.V., Kupets B., Sokolan Yu.S., Kalda G.S. Sclerometric indicators and acoustic emission activity of thermally hardened steel. Problems of Tribology 2016; 1: 6–15.
25. Shevelya V.V., Oleksandrenko V.P., Trytek A.S., Sokolan Yu.S. Scratch analysis of the formation of subsurface layers during friction of heat-treated steel. Problems of Tribology 2015; 2: 6–17.
26. Golovin I.S. Internal friction and mechanical spectroscopy of metallic materials. M.: Ed. MISiS, 2012.
27. Shevelya V.V., Kalda G.S., Sokolan Yu.S. On the connection between the relaxation and dissipative processes during steel fraction. Journal of Friction and Wear 2020; 41(2): 127–134.
28. Lakhtin Y. Engineering Materials and Metallurgy. S. Chand and Company Limited, 2006.
29. Caillard D. Dynamic strain aging in iron alloys: the shielding effect of carbon. Acta Materialia 2016; 112: 273–284.
30. Farber V.M., Selivanova O.V., Khotinov V.F., Polukhin O.N. Strain aging in steels. Ekaterinburg, 2018.
31. Shahriary M., Koohbor B., Ahadi K., Ekrami A. The effect of dynamic strain aging on room temperature mechanical properties of high martensite dual phase steel. Materials Science and Engineering A 2012; 550: 325–332.
32. Liu W., Lian J. Stress-state dependence of dynamic strain aging: Termal hardening and blue brittleness. Int. J. of Minerals, Metallurgy and Materials 2021; 28: 854–866.
33. Blanter M.S., Golovin I.S., Neuhäuser H., Sinning H.R. Internal Friction in Metallic materials A Handbook, Berlin, Heidelberg: Springer Science & Business Media, 2007.